Chapter 7

$BaTiO_3$-Based Lead-Free Electroceramics with Their Ferroelectric and Piezoelectric Properties Tuned by Ca^{2+}, Sn^{4+} and Zr^{4+} Substitution Useful for Electrostrictive Device Application

Bharat G. Baraskar, Pravin S. Kadhane, Tulshidas C. Darvade, Ajit R. James and Rahul C. Kambale

Additional information is available at the end of the chapter

http://dx.doi.org/10.5772/intechopen.77388

Abstract

Dense microstructure $BaTiO_3$ (BT) ceramic with *c/a* ~1.0144 and average grain size ~7.8 μm is developed by achieving the ferroelectric parameters Psat. = 24.13 μC/cm^2 and Pr = 10.42 μC/cm^2 with lower coercive field of Ec = 2.047 kV/cm. For BT ceramic, the "sprout" shape nature is observed for strain-electric field measurements with remnant strain ~ 0.212%, converse piezoelectric constant ~376.35 pm/V and electrostrictive coefficient Q_{33}~ 0.03493 m^4/C^2. To tune the piezoelectric properties of BT ceramic, the substitutions of Ca^{2+} and Sn^{4+}, Zr^{4+} are done for Ba^{2+} and Ti^{4+} sites respectively. The $Ba_{0.7}Ca_{0.3}Ti_{1-x}Sn_xO_3$ (x = 0.00, 0.025, 0.050, 0.075, and 0.1, BCST) system was studied with ferroelectric, piezoelectric and electrostrictive properties. The electrostrictive coefficient (Q_{33}) ~ 0.0667 m^4/C^2 was observed for x = 0.075 and it is higher than the lead-based electrostrictive materials. Another (1-X) $Ba_{0.95}Ca_{0.05}Ti_{0.92}Sn_{0.08}O_3$ (BCST) – (X) $Ba_{0.95}Ca_{0.05}Ti_{0.92}Zr_{0.08}O_3$ (BCZT), ceramics (x = 0.00, 0.25, 0.50, 0.75, and 1) is studied. The BCST-BCZT ceramic system shows the increase of polymorphic phase transition temperatures toward the room temperature by Ca^{2+}, Sn^{4+} and Zr^{4+} substitution. For BCST-BCZT system the composition x = 0.75 exhibits the d_{33}, and Q_{33} values of 310 pC/N, 385 pm/V and 0.089 m^4/C^2 respectively which is greater than BT ceramics.

Keywords: lead-free piezoelectric, $BaTiO_3$, ferroelectric, curie temperature, electrostrictive coefficient

1. Introduction

Currently, most of the electronic devices and naval departments use the materials that are based on interconversion of mechanical and electrical energies i.e. piezoelectric effect for actuator/ transducer/energy harvester applications. The examples of these devices include ink-jet printers, fuel injection actuators in cars, transducers for ultrasonic imaging and therapy in medicine, sensors and actuators for vibration control, and sonars. In many of devices, ($PbZr_{1-x}Ti_xO_3$, PZT) based piezoelectric materials are mainly employed due to its excellent piezoelectric properties viz. piezoelectric charge coefficient (d_{33} ~ *250–600 pC/N*), electromechanical coupling factor (*Kp ~ > 0.50*), mechanical quality factor (Q_m ~ 10–1000), high dielectric constant (ε_r ~ > 700), low dielectric loss (*tanδ ~ < 1%*) and high Curie temperatures (Tc ~ > 300°C). However, lead oxide (PbO), main component of PZT, is highly toxic and its toxicity is further enhanced due to its volatilization at higher temperature, particularly during calcination/ sintering and thus causing environmental pollution. Today, with increasing level of electronic equipments being manufactured, used and discarded, it has been well recognized that the level of hazardous substances (in the environment) has been rising day- to- day life. Further, Pb causes severe chronic poisoning and pain with long-term exposure (years-to-decades), even when accumulated in small traces. Therefore, to reduce environmental damage during the waste disposal of piezoelectric products as well as health hazard issues, many countries have adopted the waste from electrical and electronic equipment (WEEE), restriction of hazardous substances (RoHS) and end-of life vehicles (ELV) legislations coined by the European Union and banned the use of Pb/ PbO based materials for electronic and automobile industries. Thus, there is an open challenge to search and invent the lead-free piezoelectric ceramics and transfer them into applications in place of PZT ceramics [1]. Among the lead-free piezoelectric ceramics, perovskite-structured ferroelectrics such as $BaTiO_3$ [BT], $(Bi_{1/2}Na_{1/2})TiO_3$ [BNT], $(Bi_{1/2}K_{1/2})TiO_3$ [BKT], $KNbO_3$ [KN], $(K,Na)NbO_3$ [KNN], and their solid solutions have drawn great interest of researchers. However, there are some general problems associated with these lead-free piezoceramics such as lower Curie temperatures (T_c), or low depolarization temperatures (T_d), difficulties in poling treatments, low relative densities. For example, a) The processing of KNN ceramic has some critical issues such as volatility of alkali-oxides, compositional inhomogeneity, poor densification, and phase stability; b) $BaTiO_3$ (BT) based piezoelectric shows stable piezoelectric properties, but the main issue is of lower Curie temperature (T_c) ~ < 100°C and lower coercive field which results in more temperature dependent properties and less polarization stability as well as difficulties in poling treatments; c) BNT and BKT based ceramics have suffered from its poor sinterability and hence densification.

Barium titanate, $BaTiO_3$ (BT) is the first polycrystalline ceramic ever discovered that exhibits the stable piezoelectric and dielectric properties; hence considered as a promising lead-free ferroelectric ceramic with perovskite ABO_3 structure [2]. BT is one of the promising ferroelectric materials specifically known for its wide range of applications from dielectric capacitor to non-linear optic devices. For BT ceramic, below Curie temperature (120°C), the vector of the spontaneous polarization points in the [001] direction (tetragonal phase), below 5°C it reorients in the [011] (orthorhombic phase), and below −90°C in [111] direction (rhombohedral phase) [3–5]. The present scenario of BT based electroceramics is to

bring the polymorphic phase transition (PPT) i.e. Rhombohedral to orthorhombic (T_{R-O}) and Orthorhombic to Tetragonal (T_{O-T}) close to room temperature to achieve the phase coexistence at 300 K and hence shows the enhanced piezoelectric properties [6]. For Zr^{4+}, Sn^{4+}, and Hf^{4+} substitution at Ti^{4+} site in $BaTiO_3$ increases PPT temperatures from low temperatures (0°C and −90°C) to room temperature [6]. Recently, high performance BT-based ceramics such as $(Ba,Ca)(Ti,Zr)O_3$ (BCZT) and $(Ba,Ca)(Ti,Sn)O_3$ (BCST) prepared by substitution of Ca^{2+} at A-site and Zr^{4+}/Sn^{4+} at B-site showed the properties comparable to that of soft PZT materials [7–12]. Furthermore, the substitution of Ca^{2+}at Ba^{2+} in $BaTiO_3$-$CaTiO_3$ system (i.e. to form $Ba_{1-x}Ca_xTiO_3$ (BCT) ceramics) results in a slight increase in the Curie temperature (T_C) and on the other hand suppresses the orthorhombic to tetragonal (T_{O-T}) transition temperature. This is one of the important considerations in developing the temperature stability of piezoelectric properties for various practical applications [13]. Many research groups have reported the dielectric, diffused phase transition, ferroelectric and piezoelectric properties of BCZT and BCST ceramics [6, 7, 13–22]. However, there is a need of detailed investigation of electrostrictive properties of BT based lead free electroceramics which are correlated with the structure–property-composition having the phase coexistence of orthorhombic-tetragonal (O-T), Rhombohedral-Orthorhombic (R-O) and Rhombohedral-Tetragonal (R-T) lattice symmetries, at room temperature. Thus, in view of the above, we have investigated the ferroelectric, piezoelectric and electrostrictive properties of Ca^{2+}, Sn^{4+} and Zr^{4+} modified $BaTiO_3$ ceramics and tried to correlate the observed results with the phase coexistence of noncentrosymmetric lattice symmetries achieved at room temperature.

2. Experimental details

2.1. Synthesis

2.1.1. $BaTiO_3$ (BT) synthesis

Barium titanate, $BaTiO_3$ polycrystalline electroceramic was synthesized by conventional solid-state reaction method. Staring raw materials barium carbonate ($BaCO_3$, ≥ 99%) and titanium dioxide (TiO_2, ≥ 99%) (from Sigma Aldrich) were weighted and mixed in stoichiometric proportions and ball-milled for 15 h in the ethanol medium. After ball milling slurry were dried at 100°C overnight and dried powder grounded well. Then the powder pressed into pellets of 2 cm in diameter and 4–5 mm in thickness and calcined at 1260°C for 5 h. The calcined pellets were crushed and grounded well to form the fine powder. Thereafter, pellets with 10 mm diameter and 0.6–1 mm in thickness were prepared from calcined powder by using poly vinyl alcohol (PVA) as a binder. Finally, the prepared pellets were sintered at 1300°C for 5 h.

2.1.2. $Ba_{0.7}Ca_{0.3}Ti_{1-x}Sn_xO_3$ (BCST) synthesis

$Ba_{0.7}Ca_{0.3}Ti_{1-x}Sn_xO_3$ (BCST) ceramics with x = 0.00, 0.025, 0.050, 0.075, 0.1 were prepared by solid state reaction method. Stoichiometric amounts of AR grade raw materials of $BaCO_3$ (99%), $CaCO_3$ (99%), TiO_2 (99%) and SnO_2 (99.9%) (all are from Sigma Aldrich) were mixed

with the addition of ethanol, and dried, then calcined at 1130°C for 10 h. Thereafter, they were remixed and pressed into pellets having 10 mm diameter and 0.6–1 mm in thickness and sintered for two times first at 1260°C for 10 h and secondly at 1400°C for 5 h in an air atmosphere. The post-calcination at 1260°C for 10 h was carried out to achieve proper diffusion to assist the homogenization and avoid the phase segregation of $CaTiO_3$.

2.1.3. (1−x) $Ba_{0.95}Ca_{0.05}Ti_{0.92}Sn_{0.08}O_3$-x$Ba_{0.95}Ca_{0.05}Ti_{0.92}Zr_{0.08}O_3$ [(1−x)BCST-xBCZT] synthesis

The (1−x) $Ba_{0.95}Ca_{0.05}Ti_{0.92}Sn_{0.08}O_3$-x$Ba_{0.95}Ca_{0.05}Ti_{0.92}Zr_{0.08}O_3$ [(1−x)BCST-xBCZT] lead-free piezoelectric ceramics with x = 0, 0.25, 0.50, 0.75, 1 were prepared by mixed oxide solid state reaction. High purity analytical grade $BaCO_3$, $CaCO_3$, TiO_2, SnO_2, and ZrO_2 (Hi Media; purity ≥99%) chemicals were mixed in stoichiometric proportion and ball milled for 24 h using ethanol medium. Thereafter solutions were dried and calcined at 1200°C for 10 h in air. Calcined powders were grounded well and pressed into pellets of 1 cm in diameter and ~ 0.7–0.8 mm in thickness using 5 wt% polyvinyl alcohol (PVA) as a binder. After burning out PVA at 600°C the samples were sintered at 1350°C for 10 h.

All ferroelectric materials system investigated in this book chapter was prepared and characterized for structural information at functional ceramics laboratory, Savitribai Phule Pune University.

2.2. Characterizations

The phase formation, crystal lattice symmetry and microstructural features of the samples were examined using the X-ray diffraction (XRD) with a CuKα radiation (λ = 1.5406 Å; D8 Advance, Bruker Inc., Germany) and the scanning electron microscopy (JEOL-JSM 6306A, Japan). The relative density of sintered pellets was estimated from the ratio of the apparent density measured by Archimedes' principle and the theoretical density calculated using crystal cell parameters. For electrical property measurements, silver paste was applied on both sides of the polished surfaces of pellet and then the sample was cured at 200°C for overnight to dry out the moisture prior to any measurements. Dielectric constant (ε_r) and loss tangent (tanδ) were measured as a function of temperature from −100 to 150°C at 100 kHz using inductance-capacitance-resistance (LCR) meter (HIOKI- 3532-50, Japan), connected to a computer-controlled furnace. Polarization (*P*) versus electric field (*E*) i.e. *P-E* hysteresis loops and the electric field induced strain i.e. *S-E* curves for ceramics were recorded at Ceramics and Composites Group, DMRL, Hyderabad on virgin (unpoled) samples at an applied electric field of ~ 50–60 kV/cm at 0.1 Hz, using a ferroelectric test system (TF Analyzer 2000 of M/s. aixAcct Systems, GmbH, Germany). The piezoelectric constant d_{33} for poled ceramics was measured using piezoelectric coefficient d_{33} meter (YE2730A d_{33} meter, USA).

3. Results and discussion

3.1. High dense $BaTiO_3$ ceramic with their ferroelectric and piezoelectric properties

X-ray diffraction study confirmed the tetragonal crystal structure having c/a ~ 1.0144. The dense microstructure was evidenced from morphological studies with an average grain size ~ 7.8 μm as shown in **Figure 1(a)**. **Figure 1(b)** shows the temperature dependent variation

of the dielectric permittivity (ε_r) in the range of 25–160°C at fixed frequencies viz. 1, 25, 50, 75 and100 kHz for BT ceramic sintered at 1300°C. The phase transition from ferroelectric to paraelectric was observed at Curie temperature (T_c ~ 125°C) with ε_r = 5617 [23]. **Figure 1(c)** shows the polarization-electric field (P-E) hysteresis loops for $BaTiO_3$ ceramic measured at 0.1 Hz and room temperature. Typical hysteresis loop confirms the ferroelectric nature of the sample at room temperature. The hysteresis loop is well saturated and fully developed, indicate that external field has enough energy to switch and rotate the ferroelectric domain of BT ceramic. The saturation and remnant polarization, P_{sat} = 24.13 μC/cm^2 and P_r = 10.42 μC/cm^2 was observed at the electric field strength of 57.14 kV/cm having lower coercive field of E_c = 2.047 kV/cm. The reason for achieving improved ferroelectric properties in the present work may be attributed to the high value of c/a ratio ~1.014 and dense microstructure with average grain size 7.8 μm. The lower Ec indicate that low energy loss during electric field sweep having low energy barriers for polarization rotation i.e. soft ferroelectric nature. Low energy barrier can greatly promote the polarization rotation and effectively enhance the piezoelectric properties [3]. **Figure 1(d)** shows variation of polarization current density with respect to applied electric field. Current density exhibits the peaking behavior for both positive and negative cycle of applied electric field. The peaking behavior is a characteristic feature of the good ferroelectric ceramic having saturation polarization. Therefore, in present work we are successful to obtain the high-quality BT ceramic having saturated polarization states [23]. Thus, the observed ferroelectric properties are promising for ferroelectric memory device applications with larger P_r and P_s having low E_c. The estimated value of electric dipole moment for BT is 0.6689 × 10^{-27} C.cm by using Pr and lattice constant values.

Figure 1(e) shows the bipolar electric field induced strain curves measured for BT sample at frequency of 0.1 Hz with respect to bipolar electric fields. Sample revealed the "sprout"

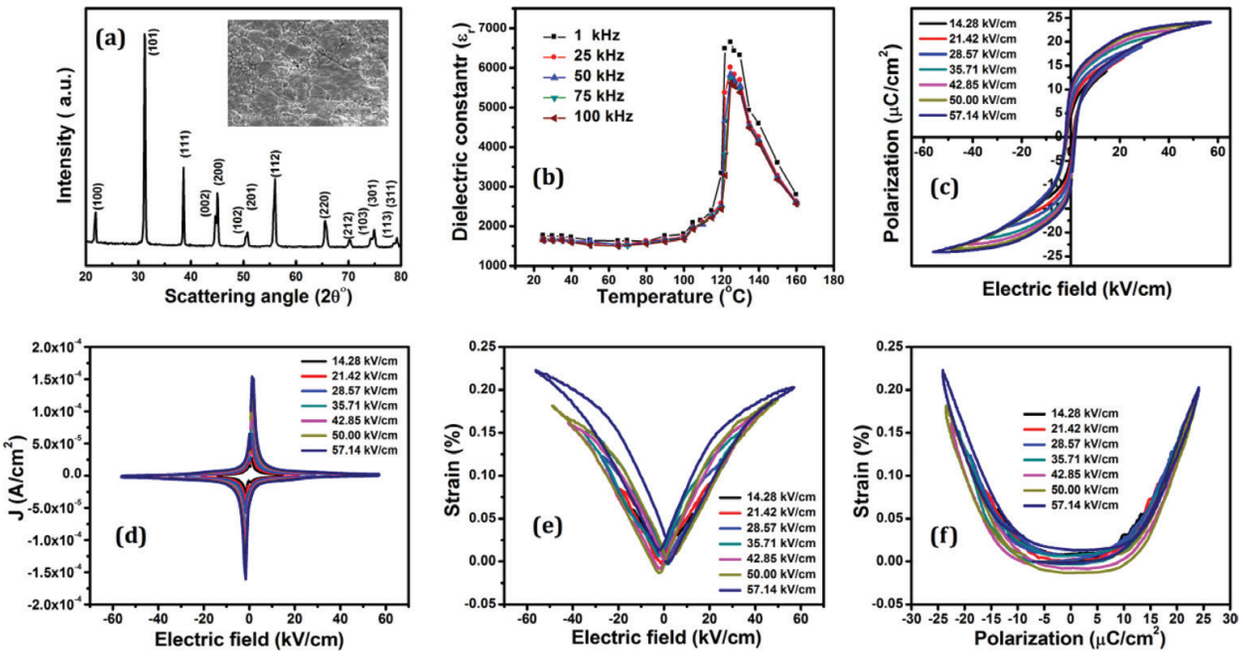

Figure 1. (a-f). (a) X- ray diffraction pattern, inset SEM, (b) relative permittivity verses temperature, (c) P-E hysteresis loop (d) J-E loop, (e) S-E loop, (f) S-P curve, of $BaTiO_3$ ceramics. (reprinted figure from ref. 23. Copyright (2016) by the AIP publishing.).

shape loop instead of "butterfly" loop which confirms the improved piezoelectric behavior [4]. Which indicates that the BT ceramic is not showing negative strain behavior, therefore here we should note that the enhancement of strain (S) is due to the sprout shape of bipolar electric field induced strain curve [4]. For electric field E = 57.14 kV/cm, better value of remnant strain 0.212% and higher value of the converse piezoelectric coefficient d^*_{33} = 376 pm/V were observed. Unfortunately, practical implementations of BT-based ceramics for commercial actuator applications are still limited by their inferior electromechanical properties as compare to those of their conventional PZT counterparts. In the present study, it is worth pointing out that the strain reaches 0.212% at E = 57.14 kV/cm which is a promising value for lead-free piezoelectric ceramic. Large value of strain output of $BaTiO_3$ is accompanied by small strain hysteresis which enabling the materials to be a promising potential for actuator applications. It is well known that domain switching and domain wall motion of $BaTiO_3$ ceramic could contribute to field-induced strain as an extrinsic effect. Since the extrinsic contribution is sensitive to external excitation, the large electric field in strain measurement may be responsible for a larger d^*_{33} = 376 pm/V [23]. Here for $BaTiO_3$ ceramic the strain-electric field hysteresis loop, which resembles the "sprout" shape loop, is may be due to the three types of effects; one is the normal converse piezoelectric effect of the lattice and other two are due to switching and movement of domain walls of $BaTiO_3$ [24]. The electrostriction coefficients Q is a four-rank tensor property that describes the relationship between polarization-induced strain (S) which proportional to the square of polarization (P) and is given by $S = QP^2$ [25]. **Figure 1(f)** shows the variation of strain with respect to polarization for $BaTiO_3$ ceramic; using this graph of strain vs. polarization we can find value of electrostriction coefficient. The relationship between field-induced strain S and polarization P satisfied equation; $Q_{33} = (S_3)/(P_3)^2$, where Q_{33} is electrostrictive coefficient, S_3 is the strain and P_3 is the polarization [4]. In our case for $BaTiO_3$ the observed value of the electrostrictive coefficient was Q_{33} = 0.035 m^4/C^2 this is larger than that of PZT (0.018–0.025 m^4/C^2) based ceramic [4]. The high Q_{33} of the BT ceramic is an important factor accounting for their high piezoelectric constant [4]. The high Q_{33} of the present BT ceramic means that it would be valuable to investigate the possible electrostrictive applications of BT ceramic.

3.2. Tune the ferroelectric and piezoelectric properties of $BaTiO_3$ by Ca^{2+} and Sn^{4+} substitution

The phase formation, microstructural aspects and dielectric properties for $Ba_{0.7}Ca_{0.3}Ti_{1-x}Sn_xO_3$ (BCST) ceramics with x = 0.00, 0.025, 0.05, 0.075 and 0.1 compositions are investigated and concluded that the compositions with x = 0.00, 0.025 and 0.05 reveals the tetragonal lattice symmetry *P4mm*, while the composition x = 0.075 shows the phase coexistence of tetragonal and orthorhombic lattice symmetries i.e. *P4mm* + *Amm2*. However, the composition x = 0.10 shows the combination *P4mm* (60%) and cubic $Pm\bar{3}m$ (40%) (ICSD# 99736) lattice symmetries which is called the pseudo-cubic (PC) lattice symmetry [26]. Thus, to invoke the improved ferroelectric and piezoelectric behavior of the material system an attempt to be made to achieve phase coexistence of noncentrosymmetric lattice symmetries near room temperature. The average grain size of BCST ceramics is found to be decreased from 8.56 to 2.36 μm with increasing Sn^{4+} content from x = 0.00 to 0.1 [26]. This is due to the lower grain-growth rates of slowly diffusing Sn^{4+} due to its higher ionic radii compared

to Ti^{4+}. Thus, incorporation of Sn^{4+} inhibits the grain growth of $BaTiO_3$ based electroceramics. To evident the phase coexistence of noncentrosymmetric lattice symmetries near room temperature the temperature dependent dielectric constant measurements were performed in the range of −150 to 150°C . Based on the dielectric anomaly observed at different temperatures with Sn^{4+} content in BCST ceramics, a phase diagram has been constructed and is shown in **Figure 2**. Thus, the observed dielectric results support the XRD results about the phase coexistence of orthorhombic-tetragonal lattice symmetry for x = 0.075 of BCST ceramics. All the BCST ceramics exhibits low dielectric loss (tanδ) < 4% in the measured temperature range.

Figure 3 (a-e), shows the polarization-electric field (*P-E*) hysteresis loop and displacement current density - electric field (*J-E*) curves measured with an applied electric field up to 50–60 kV/cm at 0.1 Hz. Both the P-E and J-E measurements were performed on virgin (unpoled) composition. All BCST ceramics exhibit a typical electric-field induced ferroelectric polarization hysteresis loop, which confirms the ferroelectric nature of investigated samples. In the present work, the compositions with x = 0.00 and 0.1 do not show the well-saturated P-E hysteresis loops. Because to achieve the saturation state of polarization in electroceramics is rather quite difficult due to the dielectric strength of the electroceramics which limits the electric field value. Moreover, the saturation state of polarization as well as the proper values of coercive field (E_c) and remnant polarization (P_r) can be reported by measuring the electric field induced displacement current density that reveals the sharp peaking behavior during positive and negative cycles [27, 28]. The presence of J-E peak corresponds to the E_c value i.e. a field responsible for domain switching for a saturated loop [27–29]. It is important to note that, most of the time, the reported values of P_r and E_c values are estimated from the observed P-E hysteresis loop which is not well saturated; thus, in principles they are not proper values as they are measured from the pre-saturated P-E loops [27, 28]. Therefore, the peak value of displacement current density (*J*) shown in **Figure 3(a-e)** for the forward and reverse cycles indicate the presence of a cyclic and uniform in both the directions, a typical characteristic of ferroelectric materials.

An observation made from **Figure 3(a-e)** reveals that the compositions with x = 0.00 and 0.1 does not exhibit the sharp peaking behavior hence they are said to be not the completely saturated, whereas the compositions with x = 0.025, 0.05 and 0.075 show the sharp peaking behavior of displacement current density. Thus, the compositions with x = 0.025, 0.05 and 0.075 are said to be completely saturated with respect to an applied electric field. Another important observation is made from **Figure 3** that for compositions with x = 0.025, 0.05 and 0.075, both the P-E and J-E curves are intersecting at a value of electric field which is approximately corresponds to the coercive field E_c. On the other hand, the compositions with x = 0.00 and 0.1 does not show any intersection of P-E and J-E plots. Furthermore, the compositions with x = 0.025, 0.05 and 0.075 exhibit the symmetric nature during positive and negative cycle of an applied electric field i.e. there is no imprint behavior of polarization state. This means that the compositions with x = 0.025, 0.05 and 0.075 may be useful for piezoelectric Ac device i.e. vibrational energy harvesting applications. The ferroelectric parameters namely remnant polarization (P_r), maximum polarization (P_{max}) and coercive electric field (E_c), with Sn^{4+} content is presented in **Figure 3(f)**. For x = 0.00 the observed values of P_r, P_{max} and E_c are 5.75 μC/cm^2, 12.70 μC/cm^2

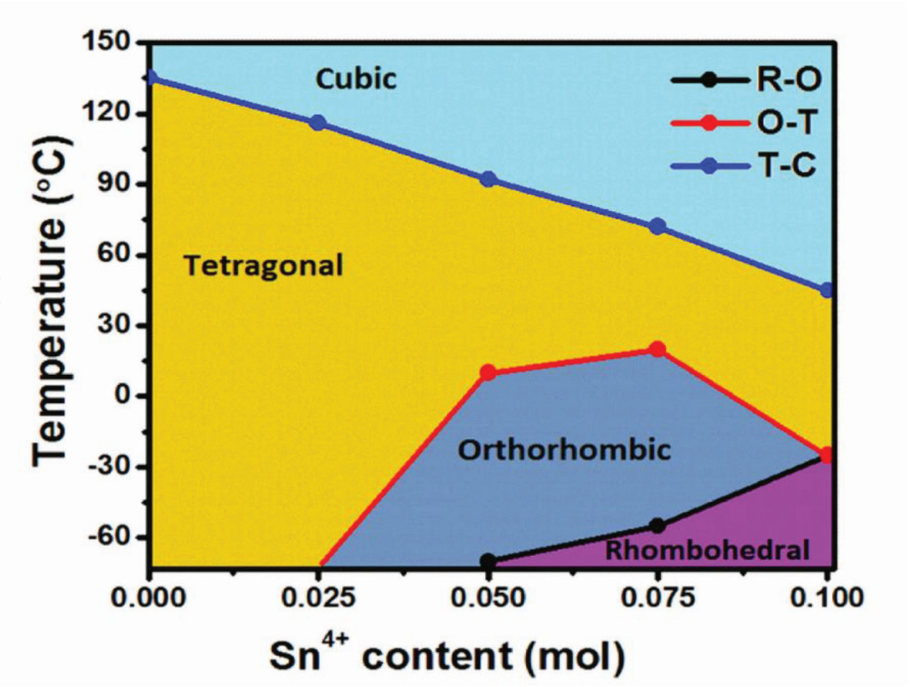

Figure 2. Phase diagram for $Ba_{0.7}Ca_{0.3}Ti_{1-x}Sn_xO_3$ ceramics. (reprinted figure from ref. 26. Copyright (2017) by the American ceramic society.).

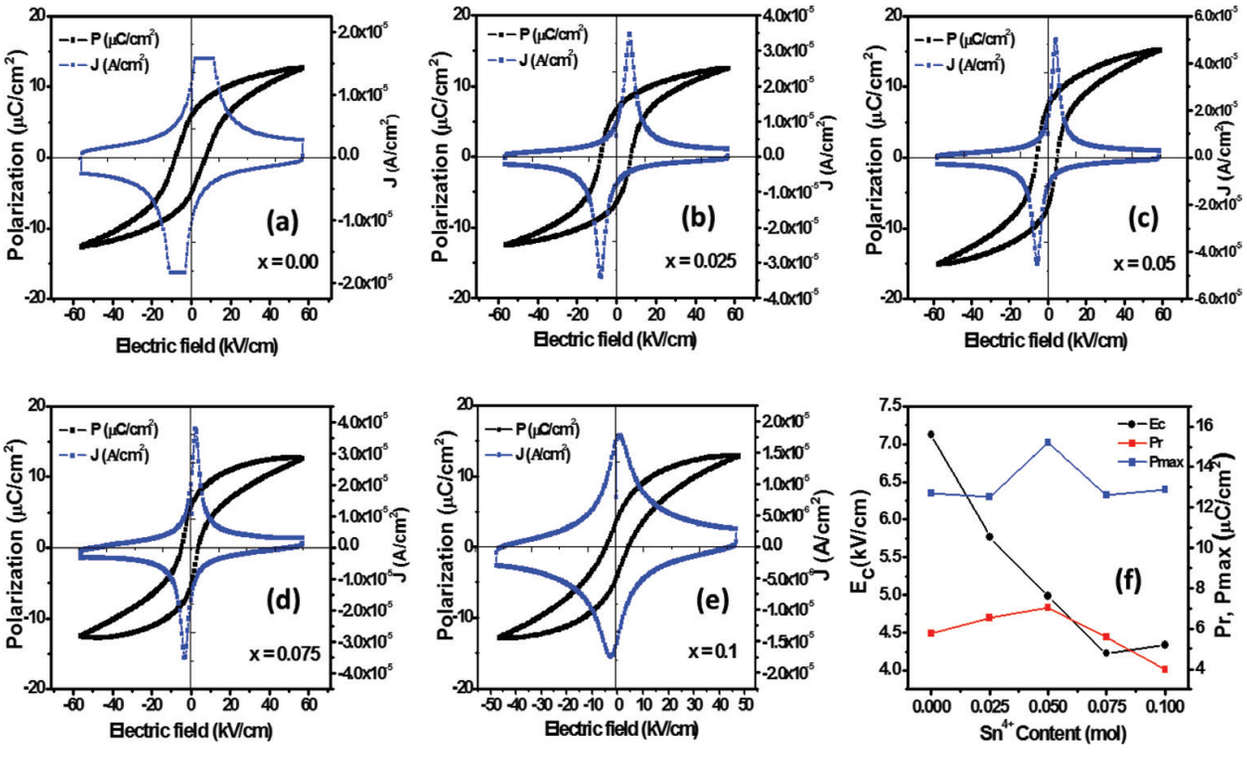

Figure 3. (a-f) (a-e) variation of polarization and displacement current density with applied electric field at 0.1 Hz for BCST ceramics, (f) variation of coercive field (E_c), remnant polarization (P_r) and maximum polarization (P_{max}) with Sn^{4+} content in BCST ceramics. (reprinted figure from ref. 26. Copyright (2017) by the American ceramic society.).

and 7.12 kV/cm, respectively. Here, the BCT showed high value of E_c which indicates that the ferroelectric domains are stabilized and thus the larger electric field is required to reverse the domains [13]. Further, as Sn^{4+} content increases from $x = 0.025$ to 0.1, the observed E_c values are in the range, 5.77–4.34 kV/cm, which indicates that these ceramics are relatively easy to pole and hence it may be possible to achieve better piezoelectric and electrostrictive properties. The possible reason for decrease of E_c with Sn^{4+} is ascribed to the decrease of *c/a* ratio with Sn^{4+} content, because the stress resulted from the domain switching gets reduced with decrease of *c/a* ratio; hence the domain switches easily under a lower electric field [30]. With Sn^{4+} content increases, the P_r increases up to 7.05 μC/cm^2 (for $x = 0.05$) and then decreases to 3.97 μC/cm^2, for $x = 0.1$. This increase of P_r values with increasing Sn^{4+} content is quite reliable, as it is known that the Sn^{4+} are not ferroelectric active whereas Ti^{4+} are ferroelectric active [16, 17, 19]. Thus, the incorporation of Sn^{4+} into $BaTiO_3$ may dilute the ferroelectricity and suppresses the piezoelectric/electrostrictive properties. However, in the present study, we have noticed the increasing trend of P_r with Sn^{4+} content up to $x = 0.05$ which could show the promising piezoelectric/electrostrictive properties. The increase in P_r and P_{max} for $x = 0.05$ may be attributed to the tetragonal crystal lattice symmetry retained in the composition. However, the compositions $x = 0.075$ and 0.1 exhibit the crystallographic phase coexistence of orthorhombic-tetragonal and pseudo-cubic lattice symmetries respectively which gives rise to the instability of ferroelectric domain and thus the P_r and P_{max} decreases [31]. Furthermore, by using remnant polarization and lattice constant values we have estimated the electric dipole moment for BCST ceramics and are found to be (0.3618, 0.4119, 0.4460, 0.3542, 0.2464) x 10^{-27} C.cm namely for x = 0.00, 0.025,0.050,0.075 and 0.1 respectively.

The bipolar strain (S) versus electric field (E) behavior was investigated for all the BCST samples and is shown in **Figure 4(a-e)**. They exhibit a typical butterfly loop, which is a feature of piezoelectric system for biaxial field. It is well-known that the butterfly loop is observed due to the normal converse piezoelectric effect of the lattice along with the switching and movement of domain walls. Here, all the BCST ceramics show the hysteretic strain behavior which may be associated with the domain reorientation. The converse piezoelectric constant is defined as $d^*_{33} = S_{max}/E_{max}$, where S_{max} is the maximum strain at maximum electric field (E_{max}); accordingly, it is calculated and shown in **Figure 4(f)**. A careful observation made on S-E plots reveals that the butterfly shape for $x = 0.00$ is not symmetric for positive and negative electric field cycle. This type of asymmetric strain behavior is not suitable for AC applications where the electric field cycles get continuously changed and hence will not work properly as desired. Therefore, an effort should be made to tailor the materials composition to get the symmetric butterfly loop with as small as deviation in d^*_{33} values for positive and negative cycles. Interestingly, in the present work, we have observed that, with Sn^{4+} content increases, the asymmetric butterfly observed for $x = 0.00$, tends to transform towards the symmetric butterfly loop for $x = 0.1$ having small deviations in d^*_{33} values for positive and negative cycles.

The average value of d^*_{33} i.e. $(d^*_{33})_{ave}$, is calculated and plotted as a function of Sn^{4+} content for BCST ceramics as shown in **Figure 4(f)**. It is observed that, as Sn^{4+} content increases the $(d^*_{33})_{ave}$ value increases linearly from 133 pm/V (for $x = 0.00$) to 199 pm/V (for $x = 0.075$) and thereafter decreases to 185 pm/V (for $x = 0.1$). The observed values of $(d^*_{33})_{ave}$ are lower compared to the reported values for Sn^{4+} modified $BaTiO_3$-$CaTiO_3$ and $BaTiO_3$ ceramics [10, 16–19, 32–34] but

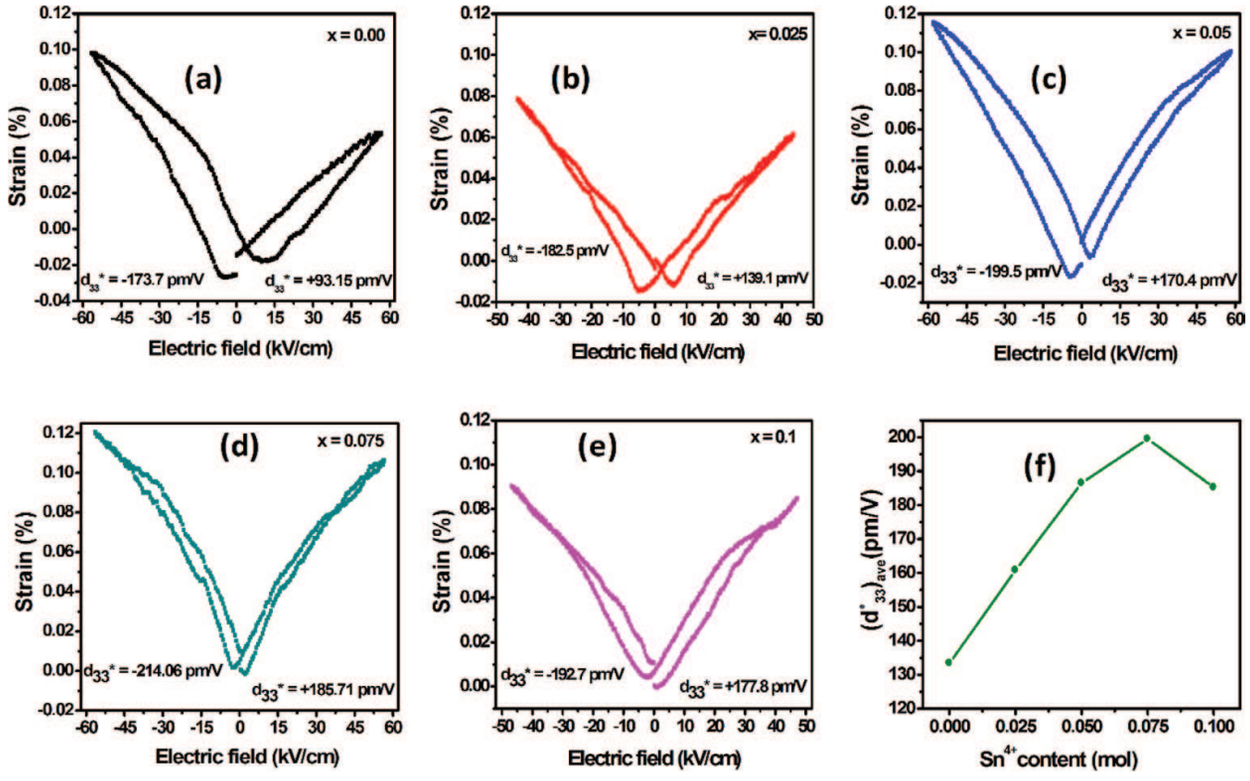

Figure 4. (a-f) (a-e) variation of bipolar electric field induced strain hysteresis loops measured at 0.1 Hz for BCST ceramics (f) variation of effective piezoelectric coefficient$(d^*_{33})ave.$ with respect to Sn^{4+} content in BCST ceramics. (reprinted figure from ref. 26. Copyright (2017) by the American ceramic society.).

it is remarkable to understand the observed symmetric and asymmetric nature of S-E butterfly loop having smaller hysteresis area. Furthermore, it can be seen from **Figure 4(a-e)** that the bipolar strain level increases from 0.097 at −56 kV/cm, 0.052% at +56 kV/cm (for $x = 0.00$) to 0.12 at −56 kV/cm, 0.105% at +56 kV/cm (for x = 0.075). The observed values of strain 0.115 at 56 kV/cm and 0.1% at 56 kV/cm for $x = 0.075$ and $x = 0.05$, respectively, are quite remarkable and comparable to the lead-based piezoelectric materials [35]. Thus, the present BCST ceramics with $x = 0.05$ and 0.075 possess the reasonably high strain level ~ 0.10 (with sprout shape rather than the usual butterfly loop) and consistently smaller area of hysteresis loop, suitable candidate for piezoelectric Ac devices [36]. The higher value of strain observed for $x = 0.075$ may be attributed to the ferroelectric orthorhombic-tetragonal phase coexistence at room temperature as evidenced from XRD and dielectric measurements. The strain as well as $(d^*_{33})_{ave}$ values observed to be decreases for $x = 0.1$ and this may be because at this composition, the system gets transformed from non-centrosymmetric to less symmetric crystal structure i.e. pseudo-cubic structure as confirmed from XRD data. The results of electromechanical investigations for BCST ceramics obtained at an applied electric field up to 50–60 kV/cm at a frequency of 0.1 Hz. The strain curves follow the square of the polarization i.e. S-P^2 as shown in **Figure 5(a-e)**, and the corresponding averaged $(Q_{33})_{ave}$ value was calculated and shown in **Figure 5(f)**. The observed S-P^2 hysteresis loop suggests that the strain and polarization are not in phase. The $(Q_{33})_{ave}$ value of lead-based electrostrictive material, such as $Pb(Mg_{1/3}Nb_{2/3})O_3$-$PbTiO_3$(PMN-PT), is reported to be about 0.017 m^4/C^2 [37]. This means that the $(Q_{33})_{ave}$

values of BCST materials are notably larger than that of the lead-based and other known lead-free electrostrictors [38–40]. Thus, the Sn^{4+} modified BCT ceramics with x = 0.05, 0.075 and 0.1 having $(Q_{33})_{ave}$ ~ 0.0469, 0.0667 and 0.0543 m^4/C^2, respectively, exhibiting the non-linear strain-polarization relation, can be registered as a promising candidate for electrostrictive actuator applications.

3.3. Tune the ferroelectric and piezoelectric properties of $BaTiO_3$ by Ca^{2+}, Sn^{4+} and Zr^{4+} substitution

Figure 6(a) shows the XRD patterns of the (1−x) $Ba_{0.95}Ca_{0.05}Ti_{0.92}Sn_{0.08}O_3$ (BCST) – (X) $Ba_{0.95}Ca_{0.05}Ti_{0.92}Zr_{0.08}O_3$ (BCZT) i.e. (1−x) BCST-xBCZT ceramics with x = 0.00, 0.25, 0.50, 0.75, and 1 measured at room temperature. All the ceramics possess the single-phase perovskite structure, and no secondary phases are detected, showing the formation of a stable solid solution between BCST and BCZT. The standard diffraction peaks cited from the tetragonal (T) $BaTiO_3$ (PDF#81-2205), the orthorhombic (O) (PDF#81–2200) and rhombohedral (R) (PDF#85–0368) are indicated by vertical lines for comparison. Sample with x = 0.00, shows the phase coexistence of O and T phases [34]. The diffraction peaks for 0.25 ≤ x ≥ 0.5 well matches with PDF#81–2200, suggesting that the crystalline structure of samples is of orthorhombic symmetry. The composition x = 1 reveals the rhombohedral phase according to PDF#85–0368. The composition x = 0.75 showed the phase coexistence of orthorhombic and rhombohedral lattice

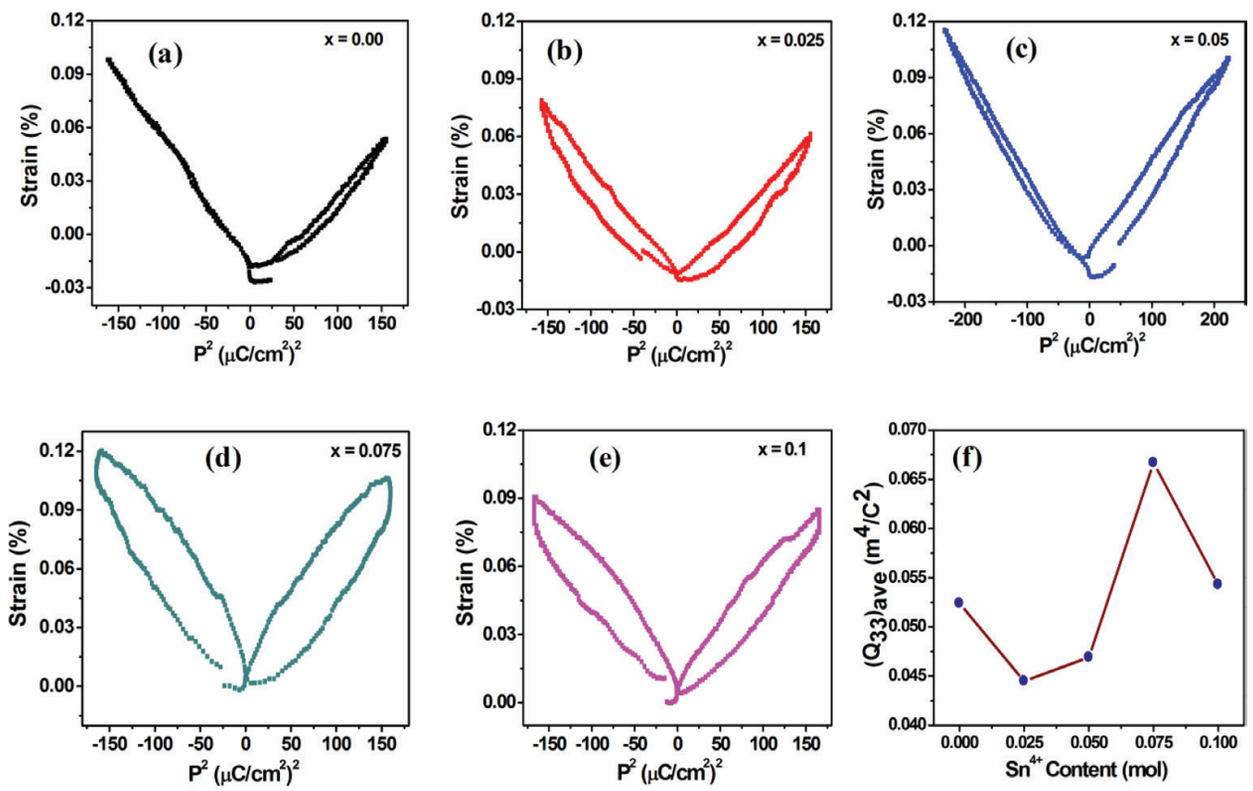

Figure 5. (a-f) (a-e) strain-polarization loops measured at 0.1 Hz for BCST ceramics (f) variation of electrostrictive coefficient$(Q_{33})_{ave}$ with Sn^{4+} content in BCST ceramics. (reprinted figure from ref. 26. Copyright (2017) by the American ceramic society.).

symmetries. The change in diffraction peak around 45° as shown in **Figure 6(b)** the gradual transitions from orthorhombic to mixed phase to rhombohedral symmetry of the unit cell at room temperature, due to the increase of x content that can be favorable to enhance the piezoelectric properties. **Figure 7** shows the temperature dependence of dielectric constant (ε_r) and dielectric loss (*tanδ*) of (1−x) BCST-xBCZT ceramics with different x, which measured at 100 kHz between −100 and 180°C. Effect of change of composition on the ferroelectric phase transitions are observed. As can be seen, (1−x) BCST-xBCZT ceramics exhibits three obvious polymorphic phase transitions corresponding to the rhombohedral to orthorhombic ($T_{R\text{-}O}$), orthorhombic to tetragonal ($T_{O\text{-}T}$) and tetragonal to cubic (T_c) respectively. The Curie temperature (T_c) is about 74°C for x = 0.00 and displays linear increasing trend up to 106°C for x = 1.00 with increasing x. This observation indicates that the Curie temperature is higher for the substitution of Ti^{4+} with Zr^{4+} than the substitution of Ti^{4+} with Sn^{4+}. It is observed that all three transitions $T_{R\text{-}O}$, $T_{O\text{-}T}$ and T_c shift to higher temperature with increase in BCZT content. Interestingly this improves Curie temperature as well as at x = 0.75 the $T_{R\text{-}O}$ observed at room temperature, provides the phase coexistence. The multiphase coexistence boundary, which has hardly any energy barrier for polarization rotation between different ferroelectric phases, is in favor of both polarization rotation and extension contributing to enhancement of piezoelectricity [41]. The observed results are in analogues to the structural analysis of (1−x) BCST-xBCZT ceramics. The dielectric constants are found in the order of 8269–9877 with lower dielectric loss in the range of 0.033–0.046, also the room temperature dielectric constant values are observed in the range of 1300–2700.

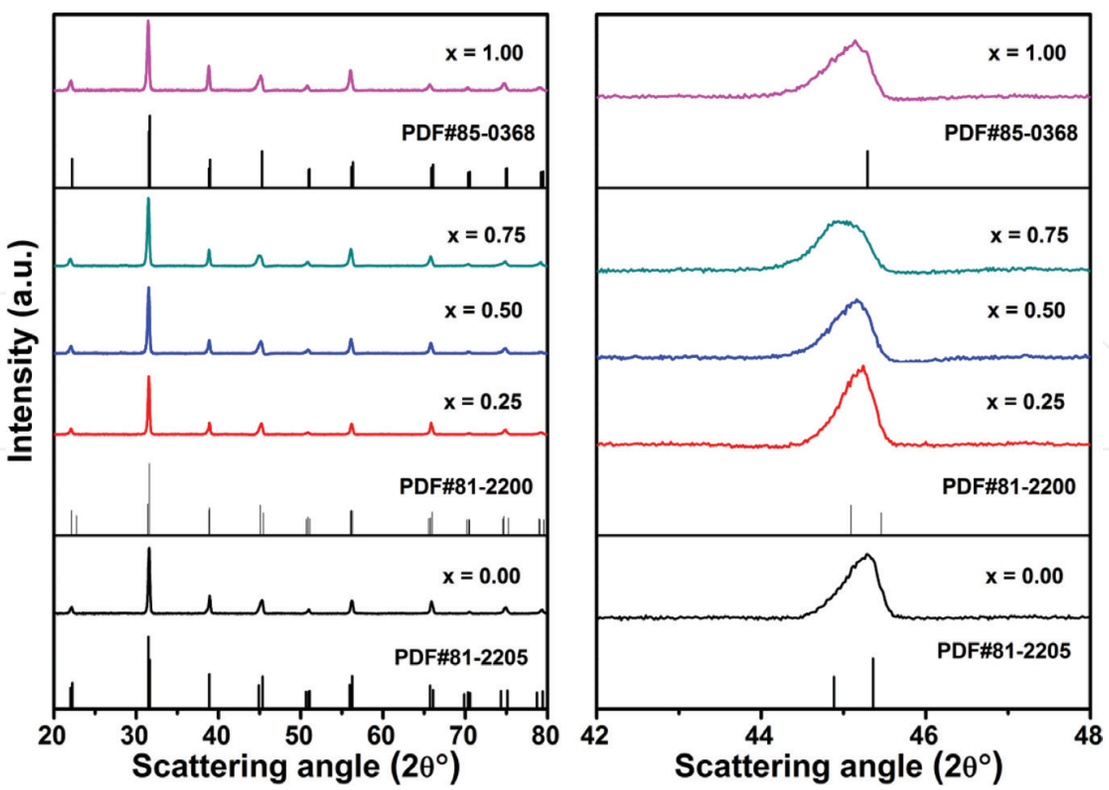

Figure 6. (a-b) (a) combined x- ray diffraction pattern between 2θ = 20 to 80° and (b) enlarged x-ray diffraction pattern between 2θ = 42 to 48°.

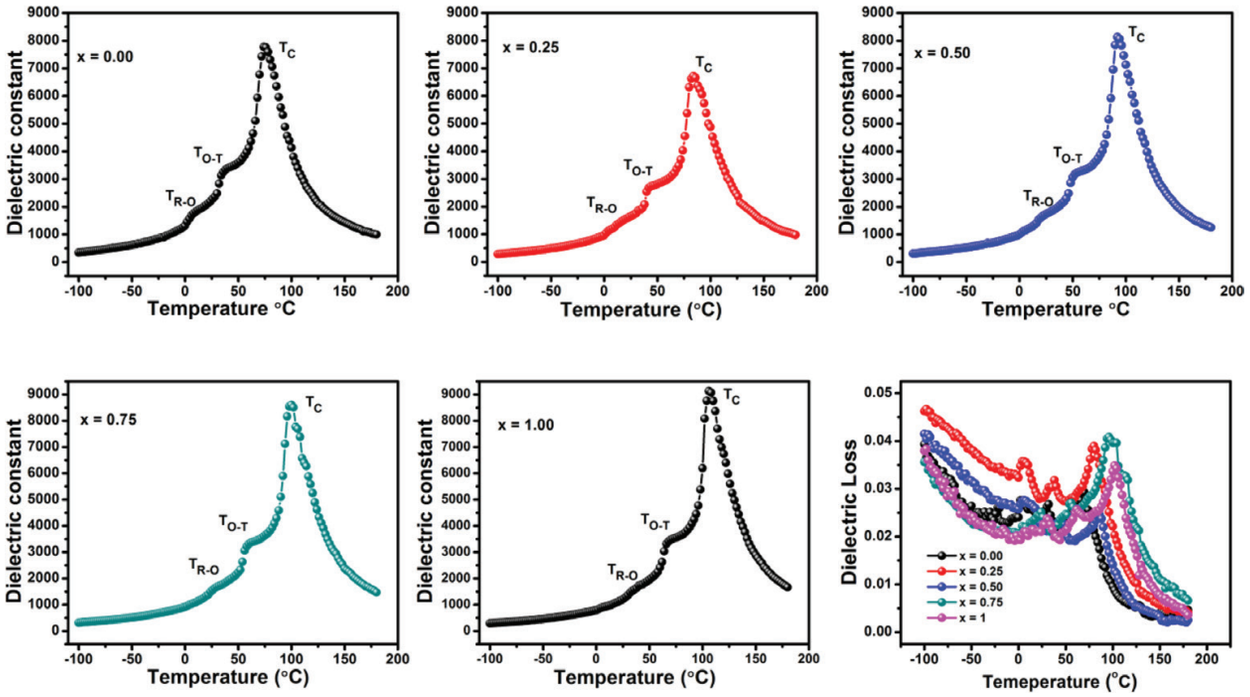

Figure 7. Temperature dependence of dielectric constant (ε_r) and dielectric loss (*tanδ*) of (1−x) BCST-xBCZT ceramics with x = 0.00, 0.25, 0.50, 0.75, and 1.

The micrograph images for (1−x) BCST-xBCZT system is shown in **Figure 8**, well densified and pore-free microstructure, consisting of irregular grains in which the large one is approximately 35 μm and the small is only about 6 μm with well-defined grain boundaries were observed. Clear grain boundary observed for ceramics samples could enhance the density and helps to improve the electrical properties of the $BaTiO_3$ based ceramics [42, 43]. All the obtained ceramics are well sintered and acquires the relative densities in the range of 93–95% with average grain size 19.4–25 μm. **Figure 9** shows the polarization versus electric field hysteresis loops of (1−x) BCST-xBCZT ceramics with different x content measured with an applied electric field up to 30–40 kV/cm at 0.1 Hz. All samples possess a typical ferroelectric polarization hysteresis loop with remnant polarization (P_r), saturation polarization (P_s) and coercive field (E_c). The ferroelectric properties, i.e. the P_r and the coercive field E_c are observed in the range of 4.7–6.6 μC/cm^2 and 2.6–3.6 kV/cm respectively. Remnant polarization increases with increase in BCZT content. Sample with x = 0.75 shows superior value of remnant polarization 6.3 μC/cm^2 with lower value of Ec = 2.9 kV/cm this can be attributed to the dipole moments of the compositions near the R-O phase coexistence being able to reorient dipoles more completely [34]. The decrease of E_c reveals that, the sample become "softer" with increase of x [10, 44]. The sample of "soft" indicates that the free energy profile for polarization rotation is anisotropically flattened at the two phases and multiphase coexistence [10]. However, Lower value of Ec indicates that the lower energy barriers are needed for polarization rotation. This lower energy barrier can greatly facilitate the polarization rotation and effectively enhance the piezoelectric properties [10, 44]. **Figure 9** shows displacement current density-electric field (J-E) curves measured for (1−x) BCST-xBCZT ceramics with an applied electric field up to 30–40 kV/cm at 0.1 Hz. All samples show sharp-peaking behavior which reveals that

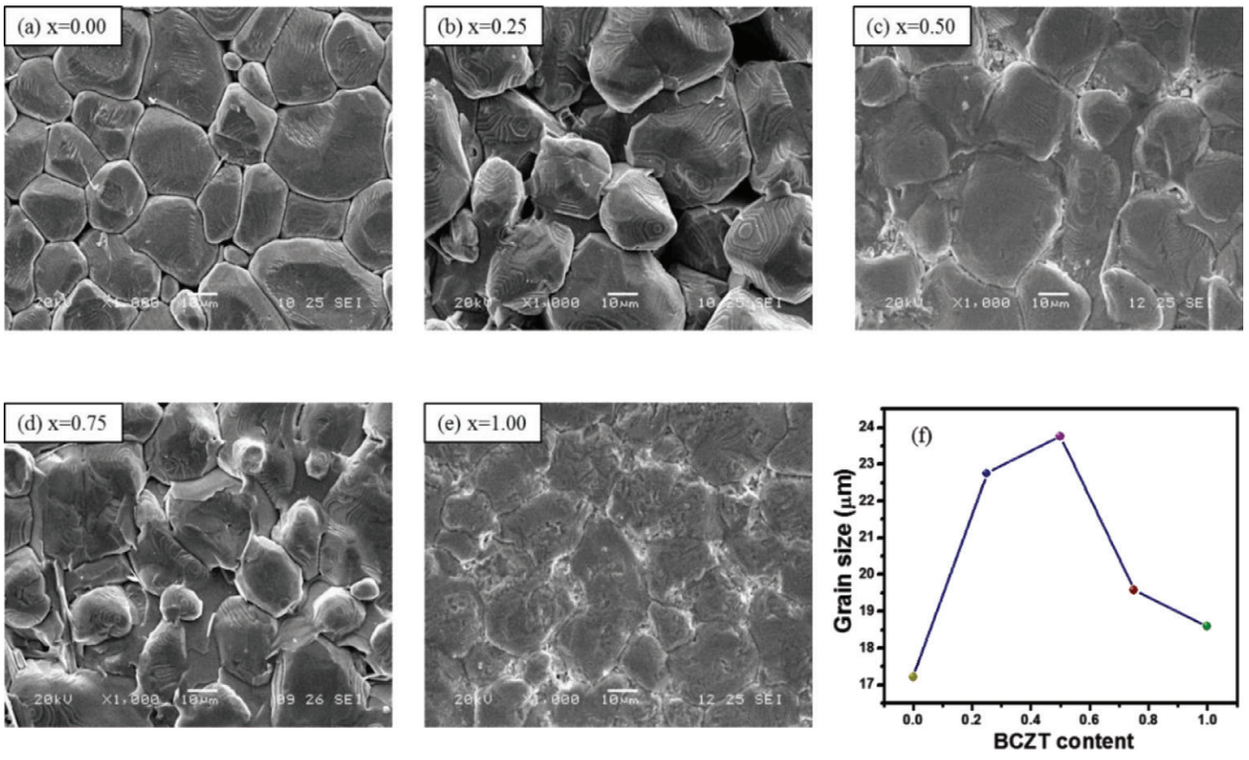

Figure 8. (a-e) SEM micrographs of (1−x)BCST-xBCZT ceramic pellets sintered at 1350°C for 10 h (f) variation of average grain size with respect to BCZT content.

samples are completely saturated with respect to applied electric field [26]. Furthermore, by using remnant polarization and lattice constant values we have estimated the electric dipole moment for (1−x) BCST-xBCZT ceramics and are found to be (0.3045, 0.3500, 0.3505, 0.4090, 0.4132) × 10^{-27} C.cm namely for x = 0.00, 0.25,0.50,0.75 and 1.0 respectively.

Figure 10 shows the bipolar field-induced strain (S-E) curves for (1−x) BCST-xBCZT ceramics measured with an applied electric field up to 30–40 kV/cm at 0.1 Hz. All samples reveal the butterfly shaped S-E loops that are typical feature of ferroelectric materials. A prominent enhancement in the maximum positive strain response from 0.086% at x = 0.00 to 0.122% at x = 0.75 is observed. In ferroelectric, electric field induced butterfly like hysteresis strain loops are occurs fundamentally due to the intrinsic and extrinsic contribution [41]. By modifying the chemical composition of $BaTiO_3$ based masteries one can achieve phase coexistence that facilitated the polarization rotation and enhance the intrinsic contribution (lattice strain) [10, 34, 41]. In ferroelectric materials the domain switching provides the extrinsic contribution, it happens when ferroelectric materials change the spontaneous polarized state along the applied electric field direction. Therefore, the higher strain S = 0.122 observed for x = 0.75 is attributed to the R-O phase coexistence. However, the extrinsic contribution is attributed to the lower value of E_c which supports to easy domain switching and contributes to achieve the superior piezoelectric properties. **Figure 10** shows variation of direct piezoelectric coefficient $(d_{33})_{ave}$ and converse piezoelectric coefficient $(d^*_{33})_{ave}$ for (1−x)BCST-xBCZT ceramics as a function of BCZT content. It can be observed that both of d_{33} and d^*_{33} curves possess a peak with increasing BCZT content. At x = 0.75, the

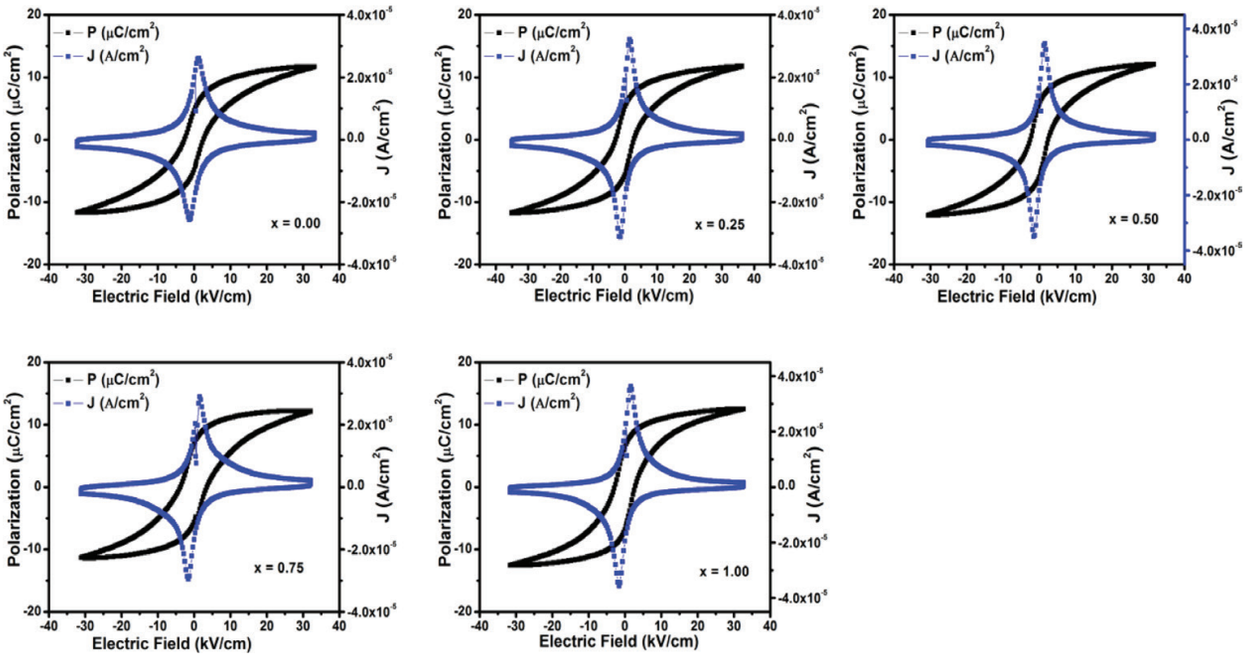

Figure 9. Variation of polarization and displacement current density with applied electric field at 0.1 Hz for (1−x)BCST-xBCZT ceramics.

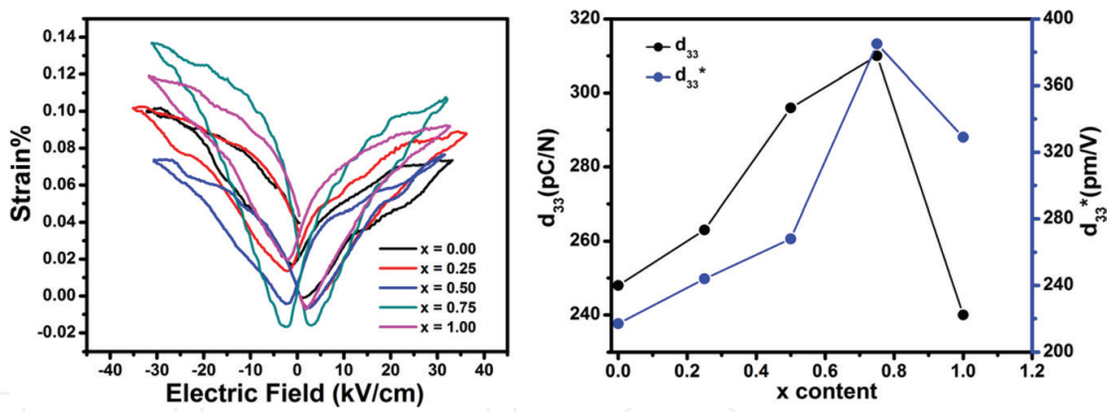

Figure 10. Variation of bipolar electric field induced strain hysteresis loops measured at 0.1 Hz, variation of direct piezoelectric coefficient $(d_{33})ave.$ and converse piezoelectric coefficient $(d^*_{33})ave.$ for (1−x)BCST-xBCZT ceramics.

higher d_{33} and d^*_{33} of the (1−x) BCST-xBCZT ceramics are 310 pC/N and 385 pm/V respectively with Q_{33} of 0.089 m^4/C^2. It is believed that the observed high piezoelectric properties should be ascribed to the phase coexistence. The O-T phase coexistence causes instability of the polarization state; therefore, the polarization direction can be easily rotated by external stress or electric field, resulting in a high piezoelectricity [10, 34, 41]. Therefore, to achieve high piezoelectric properties for lead free ceramics one has prepare samples having PPT or MPB phase compositions. The 0.25BCST-0.75BCZT ceramic sample shows the superior piezoelectric properties having moderate Curie temperature ~ 100°C can be a potential lead-free piezoelectric material to further study to replace the toxic lead based piezoelectric materials.

4. Future scope and implications

The search of lead-free piezoelectric ceramics has significantly improved over the last two decades. The deep research in ferroelectric materials can develop better ferroelectric and electrostrictive ceramics. It is necessary to develop lead free ceramic materials having morphotropic phase boundary like PZT and improve the temperature dependence of piezoelectric properties of lead free ceramics. Lower Curie temperature of BT based ceramics hinders their use in practical applications. Improvement in this regime is most welcome in the future. The improvement in piezoelectric properties of BT based ceramics has done in last few years which are attractive for various applications; though need to improve other basic properties such as Curie temperature and temperature dependent piezoelectric properties to accelerate the use of BT based materials in piezoelectric applications. It is difficult to replace the PZT by single lead free piezoelectric material. Therefore, need to develop different lead-free materials which can fulfill the different challenges and can useful for various piezoelectric applications. The BT based polycrystalline electroceramics possess inferior properties than BT based single crystal materials. In future this gap can be fulfilled by textured piezoceramics. The textured piezoelectric ceramics have potential to fulfill the gap between polycrystalline and single crystal piezoelectric ceramics. In conventional polycrystalline ceramics grains are randomly oriented while in the textured polycrystalline ceramics grain structure is oriented along one of the crystallographic direction. Due to the orientation of grain structure in specific crystallographic direction, the textured piezoelectric materials give higher performance characteristics close to single crystal materials. Also, as compare to single crystal materials the textured polycrystalline ceramics do not suffer from fracture toughness issues. In future textured BT based piezoelectric materials can become potential materials to replace the lead based piezoelectric materials.

5. Conclusions

We have successfully developed the superior quality high dense microstructure $BaTiO_3$ (BT) electroceramic material with *c/a* axial ratio of ~1.0144 having an average grain size ~7.8 μm. The BT exhibits the saturation and remnant polarization of $P_{sat.} = 24.13\ \mu C/cm^2$ and $P_r = 10.42\ \mu C/cm^2$ respectively with lower coercive field of $E_c = 2.047$ kV/cm, which is good for ferroelectric memory device applications. The concept of peaking characteristics of the polarization current density-electric field measurement is introduced to evidences the saturation state of polarization for most of the ferroelectric materials. The pure BT ceramics possesses the "sprout" shape nature instead of typical "butterfly loop" for strain-electric field measurements with remnant strain ~ 0.212%, converse piezoelectric constant d^*_{33} ~376.35 pm/V and electrostrictive coefficient Q_{33}~ 0.03493 m^4/C^2. The lead-free $Ba_{0.7}Ca_{0.3}Ti_{1-x}Sn_xO_3$ (x = 0.00, 0.025, 0.050, 0.075, and 0.1, abbreviated as BCST) electroceramic system showed the maximum electrostrictive coefficient (Q_{33}) value of 0.0667 m^4/C^2 for x = 0.075 and it is higher than some of the significant lead based electrostrictive materials. From BCST system the compositions x = 0.05 and 0.075 showed the notable electrostrictive properties that may be useful for piezoelectric Ac device applications. For (1−x) BCST-xBCZT

ceramics with x = 0.00, 0.25, 0.50, 0.75, and 1 we are successful to push the polymorphic phase transition temperatures (PPT) close to room temperature by Ca^{2+}, Sn^{4+} and Zr^{4+} substitution for BT system. For BCST-BCZT system the composition x = 0.75 exhibits the d_{33}, d^*_{33} and Q_{33} values of 310 pC/N, 385 pm/V and 0.089 m^4/C^2 respectively which is greater than BT ceramics. Thus, the piezoelectric and ferroelectric properties of BT ceramic can significantly tune by Ca^{2+} and Sn^{4+}, Zr^{4+} substitutions useful for electromechanical device application in future. Still there is a scope for BT based ceramics with Ca^{2+} and Sn^{4+}, Zr^{4+} substitutions to achieve the morphotropic phase boundary composition having giant piezoelectric properties.

Acknowledgements

RCK thankfully acknowledge the Science and Engineering Research Board (SERB)-DST, Government of India (File No. EMR/2016/001750) for providing the research funds under Extra Mural Research Funding (Individual Centric) scheme.

Conflict of interest

The authors declare that they have no conflict of interest.

Author details

Bharat G. Baraskar[1], Pravin S. Kadhane[1], Tulshidas C. Darvade[1], Ajit R. James[2] and Rahul C. Kambale[1]*

*Address all correspondence to: rckambale@gmail.com

1 Functional Ceramics Laboratory, Department of Physics, Savitribai Phule Pune University, Pune, Maharashtra, India

2 Ceramics and Composites Group, Defense Metallurgical Research Laboratory, (Ministry of Defence), Hyderabad, Telangana, India

References

[1] Rödel J, Webber KG, Dittmer R, Jo W, Kimura M, Damjanovic D. Transferring lead-free piezoelectric ceramics into application. Journal of the European Ceramic Society. 2015;**35**:1659-1681

[2] Mahesh MLV, Bhanu Prasad VV, James AR. Effect of sintering temperature on the microstructure and electrical properties of zirconium doped barium titanate ceramics. Journal of Materials Science: Materials in Electronics. 2013;**24**:4684-4692

[3] Acosta M, Novak N, Rojas V, Patel S, Vaish R, Koruza J, Rossetti GA, Rödel J. BaTiO3-based piezoelectrics: Fundamentals, current status, and perspectives. Applied Physics Reviews. 2017;**4**:041305

[4] Wang JJ, Meng FY, Ma XQ, Xu MX, Chen LQ. Lattice, elastic, polarization, and electrostrictive properties of $BaTiO_3$ from first-principles. Journal of Applied Physics. 2010; **108**:034107

[5] Li YL, Cross LE, Chen LQ. A phenomenological thermodynamic potential for single crystals. Journal of Applied Physics. 2005;**98**:064101

[6] Kalyani AK, Brajesh K, Senyshyn A, et al. Orthorhombic-tetragonal phase coexistence and enhanced piezo-response at room temperature in Zr, Sn, and Hf modified $BaTiO_3$. Applied Physics Letters. 2014;**104**:252906

[7] Liu W, Ren X. Large piezoelectric effect in Pb-free ceramics. Physical Review Letters. 2009;**103**:257602

[8] Deluca M, Stoleriu L, Curecheriu LP, et al. High-field dielectric properties and Raman spectroscopic investigation of the ferroelectric-to-relaxor crossover in $BaSn_xTi_{1-x}O_3$ ceramics. Journal of Applied Physics. 2012;**111**:084102

[9] Zhao L, Zhang BP, Zhou PF, et al. Phase structure and property evaluation of (Ba,Ca)(Ti,Sn)O3 sintered with Li_2CO_3 addition at low temperature. Journal of the American Ceramic Society. 2014;**97**:2164-2169

[10] Zhu LF, Zhang BP, Zhao L, et al. High piezoelectricity of $BaTiO_3$-$CaTiO_3$- $BaSnO_3$ lead-free ceramics. Journal of Materials Chemistry C. 2014;**2**:4764

[11] Mahesh MLV, Bhanu Prasad VV, James AR. Enhanced dielectric and ferroelectric properties of lead-free $Ba(Zr_{0.15}Ti_{0.85})O_3$ ceramics compacted by cold isostatic pressing. Journal of Alloys and Compounds. 2014;**611**:43-49

[12] Shen ZY, Li JF. Enhancement of piezoelectric constant d_{33} in $BaTiO_3$ ceramics due to nano-domain structure. Journal of the Ceramic Society of Japan. 2010;**118**:940-943

[13] Zhu XN, Zhang W, Chen XM. Enhanced dielectric and ferroelectric characteristics in Ca-modified $BaTiO_3$ ceramics. AIP Advances. 2013;**3**. DOI: 082125

[14] Wei XY, Feng YJ, Yao X. Dielectric relaxation behavior in barium stannate titanate ferroelectric ceramics with diffused phase transition. Applied Physics Letters. 2003; **83**:2031-2033

[15] Lu SG, Xu ZK, Chen H. Tunability and relaxor properties of ferroelectric barium stannate titanate ceramics. Applied Physics Letters. 2004;**85**:5319-5321

[16] Singh KC, Nath AK, Thakur OP. Structural, electrical and piezoelectric properties of nanocrystalline tin-substituted barium titanate ceramics. Journal of Alloys and Compounds. 2011;**509**:2597-2601

[17] Cai W, Fan Y, Gao J, et al. Microstructure, dielectric properties and diffuse phase transition of barium stannate titanate ceramics. Journal of Materials Science: Materials in Electronics. 2011;**22**:265-272

[18] Horchidan N, Ianculescu AC, Vasilescu CA, et al. Multiscale study of ferroelectric-relaxor crossover in $BaSn_xTi_{1-x}O_3$ ceramics. Journal of the European Ceramic Society. 2014;**34**:3661-3674

[19] Yasuda N, Ohwa H, Asano SH. Dielectric properties and phase transitions of $Ba(Ti_{1-x}Sn_x)O_3$ solid solution. Japanese Journal of Applied Physics. 1996;**35**:5099

[20] Jonker GH. Philips Technical Review. 1955;**17**:129

[21] Smolenskii GA, Isupov VA. Phase transitions in some solid solutions with ferroelectric properties. Doklady Akademii Nauk SSSR. 1954;**97**:653

[22] Shvartsman VV, Kleemann W, Dec J, et al. Diffuse phase transition in $BaTi_{1-x}Sn_xO_3$ ceramics: An intermediate state between ferroelectric and relaxor behavior. Journal of Applied Physics. 2006;**99**:124111

[23] Baraskar BG, Kakade SG, James AR, Kambale RC, Kolekar YD. Improved ferroelectric, piezoelectric and electrostrictive properties of dense $BaTiO_3$ ceramic. AIP Conference Proceedings. 2016;**1731**:140066

[24] Weaver PM, Cain MG, Stewart M. Temperature dependence of strain-polarization coupling in ferroelectric ceramics. Applied Physics Letters. 2010;**96**:142905

[25] Uchino K, Nomura S, Cross LE, Newnham RE, Jang SJ. Electrostrictive effect in perovskites and its transducer applications. Journal of Materials Science. 1981;**16**:569-578

[26] Baraskar BG, Kambale RC, James AR, Mahesh MLV, Ramana CV, Kokelar YD. Ferroelectric, piezoelectric and electrostrictive properties of Sn^{4+}-modified $Ba_{0.7}Ca_{0.3}TiO_3$ lead-free electroceramics. Journal of the American Ceramic Society. 2017;**100**:5755-5765

[27] Viola G, Saunders T, Wei X, et al. Contribution of piezoelectric effect, electrostriction and ferroelectric/ferroelastic switching to strain-electric field response of dielectrics. Journal of Advanced Dielectrics. 2013;**3**:1350007

[28] Yan H, Inam F, Viola G, et al. The contribution of electrical conductivity, dielectric permittivity and domain switching in ferroelectric hysteresis loops. Journal of Advanced Dielectrics. 2011;**1**:107-118

[29] Kumar A, Prasad VVB, Raju KCJ, et al. Poling electric field dependent domain switching and piezoelectric properties of mechanically activated $(Pb_{0.92}La_{0.08})(Zr_{0.60}Ti_{0.40})O_3$ ceramics. Journal of Materials Science: Materials in Electronics. 2015;**26**:3757-3765

[30] Fan L, Chen J, Li S, et al. Enhanced piezoelectric and ferroelectric properties in the $BaZrO_3$ substituted $BiFeO_3$-$PbTiO_3$. Applied Physics Letters 2013;**102**:022905

[31] Fu D, Itoh M, Koshihara S. Invariant lattice strain and polarization in $BaTiO_3$-$CaTiO_3$ ferroelectric alloys. Journal of Physics. Condensed Matter 2010;**22**:052204

[32] Horchidan N, Ianculescu AC, Curecheriu LP, et al. Preparation and characterization of barium titanate stannate solid solutions. Journal of Alloys and Compounds. 2011; **509**:4731-4737

[33] Xue DZ, Zhou YM, Bao HX, et al. Large piezoelectric effect in Pb-free $Ba(Ti,Sn)O_3$-x$(Ba,ca)TiO_3$ ceramics. Applied Physics Letters. 2011;**99**:122901

[34] Zhu LF, Zhang BP, Zhao XK, et al. Enhanced piezoelectric properties of $(Ba_{1-x}Ca_x)(Ti_{0.92}Sn_{0.08})O_3$ lead-free ceramics. Journal of the American Ceramic Society. 2013;**96**:241-245

[35] Lupascu DC. Fatigue in Ferroelectric Ceramics and Related Issues. New York: Springer; 2004

[36] Nath AK, Medhi N. Density variation and piezoelectric properties of $Ba(Ti_{1-x}Sn_x)O_3$ ceramics prepared from nanocrystalline powders. Bulletin of Materials Science. 2012;**35**:847-852

[37] Furuta A, Uchino K. Dynamic observation of crack propagation in piezoelectric multilayer actuators. Journal of the American Ceramic Society. 1993;**76**:1615

[38] Li F, Jin L, Xu Z, et al. Electrostrictive effect in ferroelectrics: An alternative approach to improve piezoelectricity. Applied Physics Reviews. 2014;**1**:011103

[39] Ang C, Yu Z. High, purely electrostrictive strain in lead-free dielectrics. Advanced Materials. 2006;**18**:103

[40] Zhang ST, Kounga AB, Jo W, et al. High-strain lead-free antiferroelectric electrostrictors. Advanced Materials. 2009;**21**:4716

[41] Zhu L-F, Zhang B-P, Zhao X-K, Zhao L, Yao F-Z, Han X, Zhou P-F, Li J-F. Phase transition and high piezoelectricity in $(Ba,ca)(Ti_{1-x}Sn_x)O_3$ lead-free ceramics. Applied Physics Letters. 2013;**103**:072905

[42] Li W, Xu Z, Chu R, Fu P, Zang G. Enhanced ferroelectric properties in $(Ba_{1-x}Ca_x)(Ti_{0.94}Sn_{0.06})O_3$ lead-free ceramics. Journal of European Ceramic Society. 2012;**32**:517-520

[43] Wu J, Xiao D, Wu B, Wu W, Zhu J, Yang Z, Wang J. Sintering temperature-induced electrical properties of $(Ba_{0.90}Ca_{0.10})(Ti_{0.85}Zr_{0.15})O_3$ lead-free ceramics. Materials Research Bulletin. 2012;**47**:1281-1284

[44] Xu C, Yao Z, Lu K, Hao H, Yu Z, Cao M, Liu H. Enhanced piezoelectric properties and thermal stability in tetragonal-structured $(Ba,ca)(Zr,Ti)O_3$ piezoelectrics substituted with trace amount of Mn. Ceramics International. 2016;**42**:16109-16115